

# Analysis and Design of a Microwave Coplanar Sensor for Non-Invasive Blood Glucose Measurements

María Celeste Cebedio\*, Lucas Andrés Rabioglio\*, Iván Exequiel Gelosi\*,  
Ramiro Avalos Ribas\*, Alejandro José Uriz\* and Jorge Castiñeira Moreira\*  
\*ICYTE (UNMdP - CONICET)

School of Engineering, Mar del Plata National University  
Mar del Plata, Argentina

Email: (ajuriz;casti;egelosi;avalosribas)@fi.mdp.edu.ar

**Abstract**—In this paper a design for a microwave sensor for the non-invasive measurement of blood glucose concentrations is proposed. The sensor is intended for usage as part of a non-invasive glucose-quantifying device. With this aim, three different microwave resonator structures are analyzed as possible candidates, and strengths and weaknesses are highlighted in each case. The chosen resonator is an open structure in which a finger of the patient is placed, fulfilling the role of a sample to be characterized by the sensor. The shape and size of the finger thus condition those of the resonator. Variations in the concentration of blood glucose modify the dielectric properties of the tissue, which is part of the microwave resonator-finger system, and as such, the changes translate to the resonance frequency of the whole structure. Among the three studied topologies, it was found that a single resonator designed using a coplanar structure with a ground plane showed the best trade-off in frequency sensitivity, stability and repeatability of the measurements. A notable correlation, between the resonance frequency of the proposed sensor and the blood glucose levels measured with a traditional glucometer, was found. This highlights a potential interchangeability of both glucose measurement methods.

**Index Terms**—Glucometers, Non-invasive Sensors, Microwave Resonators, Blood Glucose.

## I. INTRODUCTION

High levels of blood glucose, in people suffering from diabetes, can cause serious health problems such as blindness, kidney failure, coronary diseases, among others [1]. The risk of suffering these and other complications can be substantially reduced by the performance of a suitable control of blood glucose levels [2]. However, the traditional method for self-measurement involves the extraction of a small drop of blood from the finger, which then interacts with a reactive strip. This rather painful process can discourage users from performing adequately regular controls. For this reason, the non-invasive measurement of blood glucose has been a major goal of many companies in the last years.

Among the presently existing systems for the non-traditional measurement of blood glucose, some devices have received the *CE* mark (*European Conformity*), and/or been approved by the *FDA* (the *Food and Drugs Administration* of the United States of America), and can be found in the market.

However, attempts to produce a fully non-invasive and independent glucose meter have not yet been successful. Some non-invasive devices do exist (e.g. [3], [4]), but they are not yet recommended for independent usage, being meant for use as adjunctive devices, supplementing (but not replacing) traditional, invasive, strip-based glucose meters. Other devices have approached the measurement of blood glucose in a continuous fashion, and are referred to as CGM (Continuous Glucose Monitoring) systems [5]–[7]. These CGMs obtain measurements from interstitial fluid, and as such, require a small sensor to be placed just below the skin, which must be regularly replaced. For this reason, these devices are still rather invasive. Furthermore, readings obtained from the interstitial fluid are known to have a five to ten minutes delay with respect to the actual blood glucose level. This can be a disadvantage for individuals who take immediate action to correct dangerously high or low readings.

Aside from the currently approved devices, research on the topic of alternative glucose meters is still actively performed in recent works, utilizing varying techniques [8]–[10]. Particularly, research on the use of microwave sensors in this field has been increasing in the recent years [11]–[22]. In [11], a planar microwave resonator sensor was constructed, on top of which a finger of a user would be placed as a sample to be tested, obtaining promising results. In [12]–[14], the effects of the fingerprint and the pressure exerted by the finger on a planar sensor were studied. This approach has been extended to a substrate integrated waveguide resonator in [15]. A similar analysis was performed in [16], wherein the finger was to be placed on top of a cylindrical dielectric resonator. A microstrip waveguide structure was considered in [17], and a patch resonator in [18]. Water and glucose solutions were employed to test the applicability of a complementary split-ring resonator [19], a ring sensor structure [20], a resonator including a spiral inductor coupled with an interdigital capacitor [21], and a cross-coupled stepped-impedance resonator [22]. In every aforementioned case, a sensitivity of the microwave resonator to changes in the dielectric properties of blood, caused by modifications in blood glucose concentration, was reported.

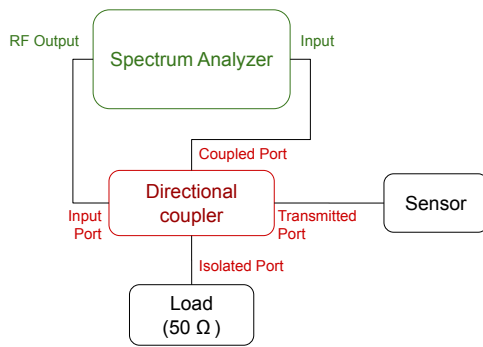


Fig. 1: Proposed system for the acquisition of the frequency response of the sensor.

With the current state of the art in mind, this paper aims to design, implement and test, a microwave sensor device usable for performing completely non-invasive, reagent-free, blood glucose measurements. A direct correlation with blood glucose levels is sought, in order to make the sensor apt for future applications as an independent (not adjunctive) device. The idea is for the sensor to consist in a structure on which a subject places their finger to perform the measurement. The working principle behind the proposed technique exploits the dependency of the dielectric constant of blood with the concentration of blood glucose, and how the former affects the resonance frequency of the resonator. In consequence, the sensor should show good properties in terms of its sensitivity with respect to changes in the electric permittivity of blood due to changes in its glucose concentration. As such, the trade-off between resonance frequency sensitivity, stability and repeatability of measurements is taken as a criterion for selecting one of the studied structures as the best suited for this implementation.

The designed microwave resonator was implemented, and its frequency response was measured by estimating the reflection coefficient over a wide range using a directional coupler and a spectrum analyzer (SA). A scheme for the proposed measurement system can be seen in Figure 1.

After performing the measurement of the resonance frequencies for various concentrations of blood glucose in a human volunteer, an analysis of the results was carried out, comparing the device with other similar approaches found in the literature.

This work is organized as follows: Section II describes the methods and planar structures used in this study; Section III is related to the design and simulation of these resonators, as well as the experiments performed on the implemented sensor; and Section IV is devoted to conclusions.

## II. METHODS

### A. Microwave sensors for blood glucose concentration measurements

It has been studied that variations in glucose concentration cause changes in the electromagnetic properties of blood, specifically, in its permittivity. It has also been proven that

the dielectric properties of blood are modified because of changes in blood glucose levels in a greater extent than due to changes of other compounds present in them [21], [23]. These variations can be detected by a microwave sensor, since its frequency response can be associated with the dielectric properties of the materials that interact with it [10].

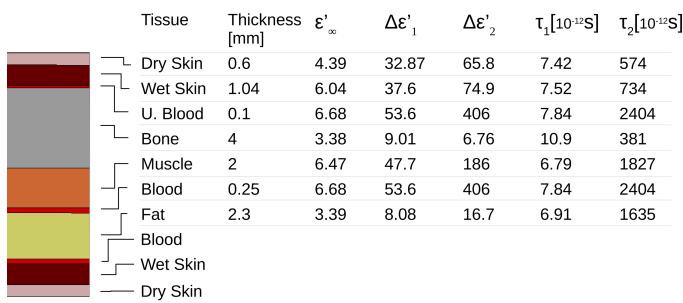
For the purposes of precision, compactness, direct detection, real-time sensing and label-free characterization, a resonator is a type of electromagnetic sensor well suited for this application [22]. Such devices have shown promise for non-invasive monitoring in bio-medical applications [13], [14]. Furthermore, the proposed microwave sensor is aimed to be a part of a complete glucose meter. Such a device should include the required measurement equipment to estimate the magnitude of the  $S_{11}$  scattering parameter (a reflection coefficient [24]) as a function of the frequency. This is because a minimum in this function implies the existence of an increased amount of energy being stored in the structure, in other words, a resonating behavior. The effect of the properties of the biological sample that interacts with the resonator is enhanced at these frequency values, due to the increase in stored energy. As such, although the entire frequency response is affected, at some level, by the properties of the sample, this effect is greater (and more easily measured) at the resonance frequencies.

The gold standard method for the determination of blood glucose concentration is known as the Hexokinase method. This procedure involves the extraction of a 1.5 mL blood sample, and its analysis in a laboratory using specialized equipment [25]. The resulting data is considered free of error. However, the most widespread way of testing blood glucose is the use of capillary glucometers, where a test strip interacts with a drop of blood, extracted by pricking the finger. This method is invasive as well, and it requires a constant supply of reagents, since the test strip is discarded after each use. Also, this measurement is not without error, with results being within  $\pm 15\%$  accuracy most of the time. The advantage of this method is that it can be performed directly by the user, on demand, and it provides real-time information. The proposed, microwave method would present these same advantages, with the addition of being non-invasive and reagent-free. As such, a limitation of this device would be the possibility of error in a blood glucose reading. An important objective for the proposed design is to provide a good accuracy.

Recent works have focused on the finger as a convenient and feasible sample to interact with the resonator [13], [15], [16]. Since simulation methods are suitable as design tools for microwave sensors, and the tissues are part of the microwave resonator-finger system, an adequate model of the biological sample to be sensed has proved necessary.

### B. A multi-layer model for biological tissues

A multi-layer approach is proposed to represent the little finger as a biological sample. This type of model has been used in physiological measurements to facilitate and assess the feasibility of the detection of changes in dielectric properties in the different layers of the tissue under study [23], [26]–[29].



Tissue	Thickness [mm]	$\epsilon'_{\infty}$	$\Delta\epsilon'_1$	$\Delta\epsilon'_2$	$\tau_1[10^{-12}\text{s}]$	$\tau_2[10^{-12}\text{s}]$
Dry Skin	0.6	4.39	32.87	65.8	7.42	574
Wet Skin	1.04	6.04	37.6	74.9	7.52	734
U. Blood	0.1	6.68	53.6	406	7.84	2404
Bone	4	3.38	9.01	6.76	10.9	381
Muscle	2	6.47	47.7	186	6.79	1827
Blood	0.25	6.68	53.6	406	7.84	2404
Fat	2.3	3.39	8.08	16.7	6.91	1635
Blood						
Wet Skin						
Dry Skin						

Fig. 2: Model and parameters of the little finger. Three blood layers of different thickness are modeled.

Recent studies have proposed different multi-layer models for the human finger, comprised of the biological tissues known as fat, skin, blood and bone [12], [16]. However, these studies have not specified the reason behind the choice of the thickness of each layer. For this study, a characterization of the little finger was performed using ultrasound technology. This was done in order to estimate realistic values for layer thickness.

The physical characterization of each layer was performed with the collaboration of professionals who, through the use of ultrasound measurement equipment, were able to estimate the thickness of each layer from the little finger of a human volunteer. These layers were assumed to be homogeneous. After modeling the multi-layer structure, the electromagnetic properties of the tissues were specified according to the second order Debye approximation in Equation 1, using parameters in [28] for the 500 MHz to 20 GHz range. A drawing of the layers and their parameters can be seen in Figure 2.

$$\epsilon_r^*(\omega) = \epsilon'_{\infty} + \sum_{n=1}^2 \frac{\Delta\epsilon'_n}{1 + j\omega\tau_n} \quad (1)$$

The proposed model considers ten layers, with six different biological tissues: dry and wet skin, bone, muscle, fat and blood. Blood is a liquid connective tissue that is present in capillaries, veins and arteries scattered throughout the living tissue. In this case it was modeled in the shape of three thin layers, distributed among the other layers. This representation was considered more realistic than the approach found in the aforementioned published works, wherein the modeling of a single, thick blood layer had been proposed. Likewise, the skin was differentiated into two layers of different thickness and dielectric properties.

The different thickness values, estimated by the aforementioned ultrasound equipment, are shown in Figure 2. These values are used for the simulations, although it is expected that different users should display slight variations in the thickness of each layer, particularly with gender and age [10].

### C. Planar structures

A suitable structure for a microwave resonator would be one for which changes in the dielectric properties of the sample (in this case, the finger, and its model in simulations) translated

into significant changes in the response of the sensor to be implemented. As such, an important consideration for the designed microwave resonator was its electromagnetic field distribution, which defines the intensity of its interaction with the sample under test. The finger then becomes a part of the resonator, modifying the original unloaded electromagnetic field distribution.

In a resonator, the electromagnetic and physical properties (permittivity, conductivity, size, etc.) of the material under test determine how it interacts with the excited field lines. Therefore, if the sample underwent any changes in its dielectric properties, these would be reflected in a modification of the field lines of the resonator, which would then translate into changes to the measurable variables that define the structure (impedance, resonance frequency, etc.). The depth of penetration and the orientation of the electromagnetic fields lines depend on the operating frequency and the shape of the resonator, among other factors. Consequently, these aspects are considered first in the design.

There is no settled choice of frequency for non-invasive glucose monitoring using microwave resonators. Most of the systems found in the literature choose on the frequency for pragmatic issues related to size or cost of the device. Generally, lower frequencies achieve greater tissue penetration than higher ones, because of the inherent conductivity of the biological tissues [10]. For this paper, frequency values in the 1.5 to 2.5 GHz interval are chosen, lower than most previous studies, which focus on the 3 to 10 GHz range. This is done in order to achieve sensitivity to blood glucose variations by increasing tissue penetration, while also making several 3 GHz instruments available for use in this research.

Concerning the shape of the sensor, for a multi-layer model of the little finger, a planar resonator structure is particularly well suited. A circuit printed with this technique would irradiate the excited electromagnetic field into the finger, which would rest laying on the resonator. For this reason, the conformal mapping technique presented in [30] is useful to design a complete planar sensor that accounts for the finger as well. This method was designed to calculate the effective permittivity and impedance of a multi-layer coplanar waveguide (CPW) or microstrip line (MSL). In this case, a single substrate layer is proposed, but the multi-layer finger model placed on top of it would act as additional dielectric layers.

The multilayer waveguide conformal mapping method was utilized to calculate the dimensions of the sensors of interest. This provided approximate values for the design. Following the calculation of the parameters, these were tuned using the *CST Studio* software [31]. The distribution of the electromagnetic fields for three common types of planar structures, MSL, CPW, and coplanar waveguide with ground plane (GCPW), was analyzed.

In all cases, FR-4 substrate was employed [32], displaying the following properties: 1.6 mm thickness, relative permittivity of 4.3 (at 1 GHz), loss tangent of 0.02, copper thickness of 35  $\mu\text{m}$ .

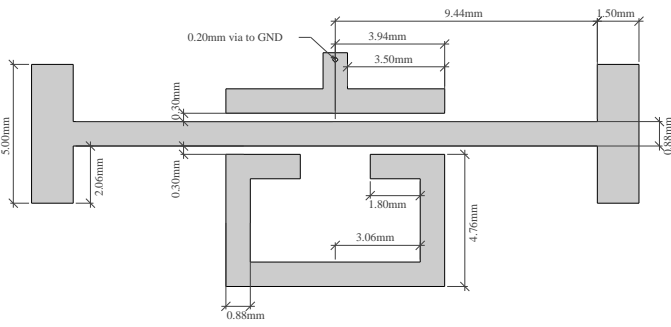


Fig. 3: The proposed MSL sensor. Top layer view; bottom layer is a continuous ground plane.

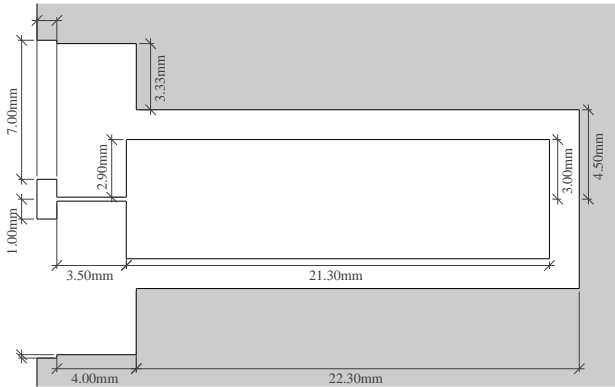


Fig. 4: The proposed CPW sensor. Single layer.

The selected MSL topology was a band-stop filter constituted of three coupled lines. The scheme was similar to the one considered in [33], but with the introduction of an additional transmission zero as described in [34]. The resulting filter would have a narrower bandwidth. This was done in order to increase the penetration of the field lines in the area where the sample was placed. Next, the effective permittivity and trace impedance were calculated using the equations derived in [30]. These allowed to determine the resonance frequency of the sensor, and the parameters were iterated upon until it reached 1.6 GHz, which is in the range of interest. The dimensions of the MSL are detailed in Figure 3.

Next, a CPW topology was developed, following a similar approach. A single, straight conducting line was used to begin, with width chosen arbitrarily. Again, the effective permittivity and trace impedance were calculated using the equations in [30]. With these, the wavelength was determined for a desired resonance frequency of 1.8 GHz. The length of the trace was set to be equal to half a wavelength. This introduced an open circuit condition at that exact frequency, encouraging the resonance phenomenon. The input trace was tuned in order to improve the simulated impedance. The dimensions of the modeled CPW can be observed in Figure 4.

Finally, the GCPW was designed. The equations in [30] were used for a regular CPW of 5 mm trace width and 2.5 mm gap. Considering the tissues in the finger as additional substrate layers, this indicated a relative effective permittivity

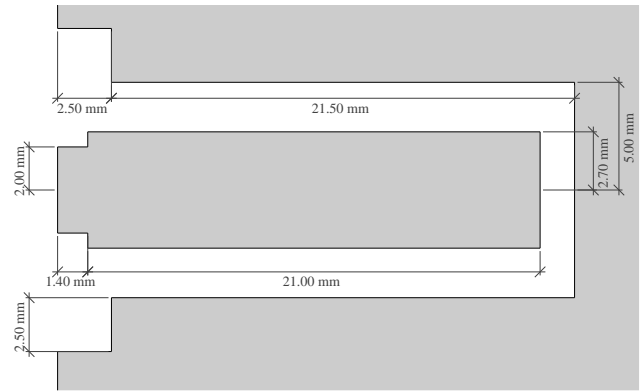


Fig. 5: The proposed GCPW sensor. Top layer view; bottom layer is a continuous ground plane.

of  $\epsilon_{ef} = 14.6$  and trace impedance  $Z = 22.6 \Omega$ . This implied a wavelength of  $\lambda = 43.6$  mm at 1.8 GHz. A half wavelength trace would resonate at that frequency. Next, the bottom ground plane was added, completing the GCPW. This slightly shifted the value of the resonance frequency, so the dimensions were tuned during simulations to compensate, finally obtaining the topology detailed in Figure 5. The input trace was also tuned in order to improve the simulated impedance.

### III. IMPLEMENTATION AND RESULTS

#### A. Characterization of the proposed microwave structures

The designed planar structures were first compared with each other, according to different desired or undesired behaviors. Using the simulation environment, different modifications were introduced to the structures to observe their effects.

In Figure 6 the simulated frequency response of the scattering parameters of the three modeled topologies is shown. The frequency of a resonance mode can be measured from a minimum in each  $S_{11}$  reflection parameter curve for the CPW and GCPW sensors. In the case of the MSL filter, the band-stop frequency is measured observing the  $S_{21}$  transmission parameter. The figure also shows the variation of each curve to changes in the  $\Delta\epsilon'_1$  parameter of the permittivity of every blood layer. It can be appreciated that the resonance frequencies are susceptible to these changes, and this is the measurement principle. The  $\Delta\epsilon'_1$  parameter was swept from 30 to 70 (the regular value being 53.6). This range, according to [23], was considered ample enough to include variations from 0 to 16000 mg/dL in blood glucose. Although such extreme values are unrealistic, it would imply a correct operation when considering realistic values (rarely below 70 or over 500 mg/dL even in disorderly cases). The range of variation of the  $\Delta\epsilon'_1$  parameter in simulations was wide. This was done in order to provide considerable resonance variations for the comparison of the three planar structures. This would help validate the operation of the sensors in a wide range of frequencies. It can also be appreciated that the quality factor  $Q$  varies with each case. This phenomenon is caused by the imaginary part of the complex relative permittivity, which is affected by the wide sweep in  $\Delta\epsilon'_1$ .

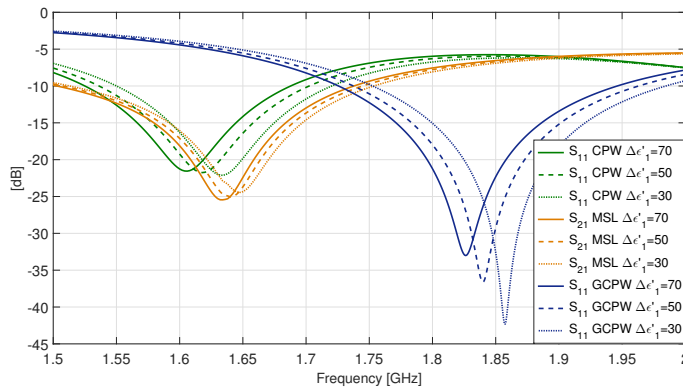


Fig. 6: Simulated spectroscopy comparison of the three topologies under study, showing resonance frequency variation in each case due to changes in the  $\Delta\epsilon'_1$  parameter in blood. Characterization is performed using the  $S_{11}$  parameter for the CPW and the GCPW, and the  $S_{21}$  parameter for the MSL.

TABLE I: Comparison of sensitivity parameters.

Sensitivity	MSL	CPW	GCPW
$\Delta f / \Delta h_{ps}$ [MHz/mm]	-371	-105	-134
$\Delta f / \Delta W$ [MHz/mm]	-3.6	-11.9	-1.5
$\Delta f / \Delta\epsilon'_r$ [MHz]	-0.4	-0.96	-0.92
$\Delta f_c$ supp. [MHz]	43.5	168	75.1
$\Delta f / \Delta\epsilon'_r$ supp. [MHz]	-0.39	-0.85	-1.04

The quotient  $\Delta f / \Delta P$  was employed as a measure of relative variation, or sensitivity, to each parameter of interest, where  $\Delta f$  is the resonance frequency variation, and  $\Delta P$  is the variation of the parameter under analysis. Parameters taken into account in the comparison were the sensitivity of the resonance frequency of the whole structure to changes in the permittivity of the layer of blood; and the invariance of the same parameter to undesired changes, such as shape, position and height of the layers of the sample model. Table I shows a comparison of the structures under study, using different sensitivity parameters. The variations considered are:

- $\Delta f$ , absolute variation in the resonance frequency.
- $\Delta h_{ps}$ , absolute variation in the dry skin layer thickness.
- $\Delta W$ , absolute variation in the width of the sample.
- $\Delta\epsilon'_r$ , absolute variation in the  $\Delta\epsilon'_1$  parameter of the permittivity of the blood layer.
- $\Delta f_c$  supp., absolute shift in the original central frequency of the structure when adding the support.
- $\Delta f / \Delta\epsilon'_r$ , relative variation of the central frequency with respect to changes in the  $\Delta\epsilon'_1$  parameter of the permittivity of the blood layer, specified both before and after adding an acrylic fixing support (“supp.” suffix).

In Figure 7 a simulation of the intensity of the electric field is shown, for the CPW resonator and inside the first blood layer, at the resonance frequency. The  $dB_{max}$  units shown are relative to the maximum electric field intensity present at the feeding wave port. The corresponding  $V/m$  values are dependent on input power. In this case, the electric field showed its greatest concentration near the wave port, and

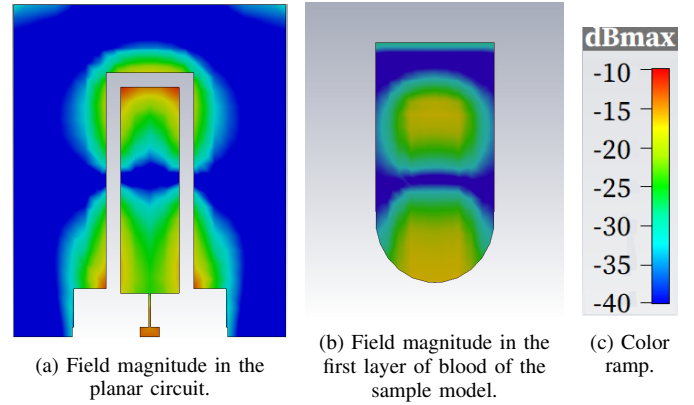


Fig. 7: Electric field intensity in the CPW sensor. Scaling in  $dB_{max}$  is relative to the maximum field strength at the feeding wave port.

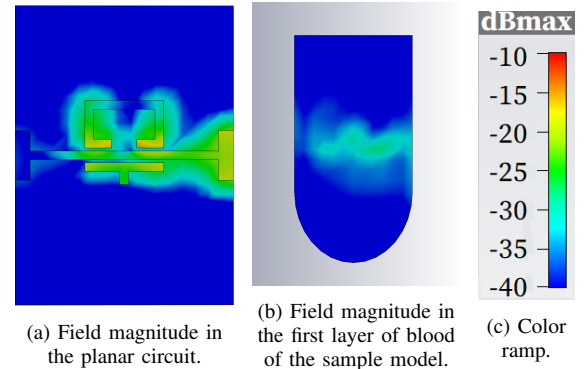


Fig. 8: Electric field intensity in the MSL sensor. Scaling in  $dB_{max}$  is relative to the maximum field strength at the feeding wave port.

close to the open circuit termination. The strip measures half a wavelength at this frequency, so the electric field direction in one maximum is opposite in the other. As seen in Table I, the CPW structure was highly sensitive to changes in the permittivity of the blood layer. This was attributed to the overall strong intensity of the electric field that can be observed in the nearest layer corresponding to blood tissue. However, this property also increased sensitivity to any changes occurring in the geometry of the proposed structure, which was undesired. This behavior was observed in Figure 6, where the resonance frequency of the simulated CPW resulted in approximately 1.6 GHz when the designed one was 1.8 GHz. It was also observed that the added support produced a considerable decrement in the sensitivity to the desired parameter.

In Figure 8 the intensity of the electric field is shown for the MSL filter and inside the first blood layer, at the resonance frequency. It can be observed that electric field lines are concentrated in the input and middle section of the MSL drawing. This is because the measurement frequency corresponds to the central stop frequency, where output is minimum. Due to the low penetration of electric field lines into the blood layer, this structure proved to be less sensitive to its permittivity than the alternatives.

In Figure 9 the simulated intensity of the electric field is

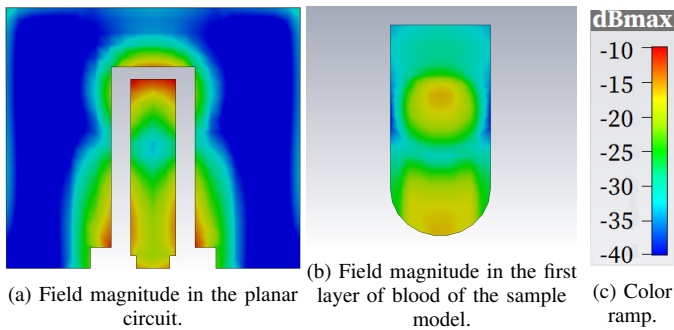


Fig. 9: Electric field intensity in the GCPW sensor. Scaling in dBmax is relative to the maximum field strength at the feeding wave port.

shown, for the GCPW structure. As was the case for the CPW, the electric field lines have their greatest concentration near the wave port and the open circuit termination, but in a greater magnitude relative to the input power. This can be appreciated in the intensity of the red color in Figures 7 through 9. The overall sensitivity to the permittivity of the blood layer was comparable to that of the CPW, as observed in Table I. Furthermore, this topology introduced a considerably better stability to the  $\Delta W$  parameter.

The analysis carried out concluded that the GCPW structure had several advantages over the others presented. The addition of the acrylic medium made it the most sensitive to changes in the permittivity of the layer of blood. The sensitivity to variations in the thickness of the skin layer was lower than the MSL and comparable to the CPW. Furthermore, changes in the width of the whole finger produced the lowest disturbance in the GCPW. Another advantage was the relative simplicity of its implementation, especially when compared to the MSL.

In Figure 10 a detail of the simulated frequency response of the  $S_{11}$  scattering parameter of the GCPW sensor is shown. The overall resonance frequency is around 1.84 GHz, which is near the 1.8 GHz assumed in calculations. A total resonance frequency variation of 31.2 MHz can be appreciated between limit parameter values (30 and 70). The quality factor varied for a total of 202 units (from 123 to 325).

In order to quantify the potential error due the positioning of the finger on the resonator, a 2 mm displacement of its model was performed in every coordinate direction. The change in the resonance frequency was recorded. A maximum shift of 100 MHz took place when moving the finger  $\pm 2$  mm in a direction parallel to the conducting line. When the movement was in the perpendicular direction, an increase of 30 MHz was recorded. This is comparable to the amounts reported in [14] and [15] (150 and 130 MHz respectively), but higher than the one simulated in [16] (15 MHz), although the finger models used by these authors were different.

### B. Experimental validation of the designed GCPW sensor

A picture of the implemented prototype is shown in Figure 12. The acrylic support on which the GCPW sensor is placed can be appreciated. The molded white plastic container was personalized for the little finger of a non-diabetic volunteer, in

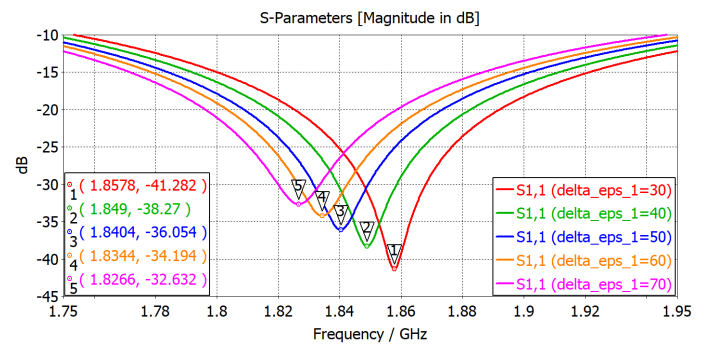


Fig. 10: Simulated frequency response ( $S_{11}$  parameter of the GCPW sensor plus the finger model) for different values of the  $\Delta\epsilon'_1$  parameter for the permittivity in the blood layers.

order to fixate the sample and minimize possible discrepancies in each measurement due to its position.

The employed SA was the HP8594E, setup to sweep frequency values from 1.8 to 2.3 GHz, using an intermediate frequency (IF) bandwidth of 1 MHz and video bandwidth of 300 kHz. The SA was equipped with a  $-10$  dBm tracking generator, which was used as signal input. The validation was performed as follows:

- 1) The reflection coefficient was estimated by using the SA and a 778D dual directional coupler. The resulting frequency response curves were saved.
- 2) The volunteer had a meal of high glycemic index.
- 3) Using an Accu-Chek Performa glucometer, blood glucose levels were recorded.

Steps 1) and 3) were carried out simultaneously every few minutes, for eighty minutes. This amount of time was considered for the blood glucose levels to begin decreasing. The sensor was kept at room temperature and humidity, which remained constant throughout the length of the experiment. Contact with the human body was brief, for only a couple of seconds, so as to avoid heat transfer to the sensor. The body temperature of the healthy volunteer also remained unchanged.

Three of the measured  $S_{11}$  curves are shown in Figure 11. For comparison purposes, three of the simulated curves were added, for different values of blood permittivity. The overall resonance frequency of the implementation was higher than in simulations (around 2.1 GHz, rather than 1.84 GHz). The  $Q$  factor was also notably lower in experimental measurements (average of 20 instead of 238). These discrepancies were attributed to the model of the finger, which, although based on ultrasound data, remains a simplification of a real finger. The variations in the resonance frequency during the experiment were also considerably higher than in simulations (121 MHz from lowest to highest, rather than 31.2 MHz). This phenomenon has been reported in the past, signaling differences in the dielectric characterization of blood *in vitro* and the behavior *in vivo* [20].

A time line of this experiment is shown in Figure 13. As seen, the resonance frequency of the finger-sensor system evolved in a notably similar manner to the levels of blood

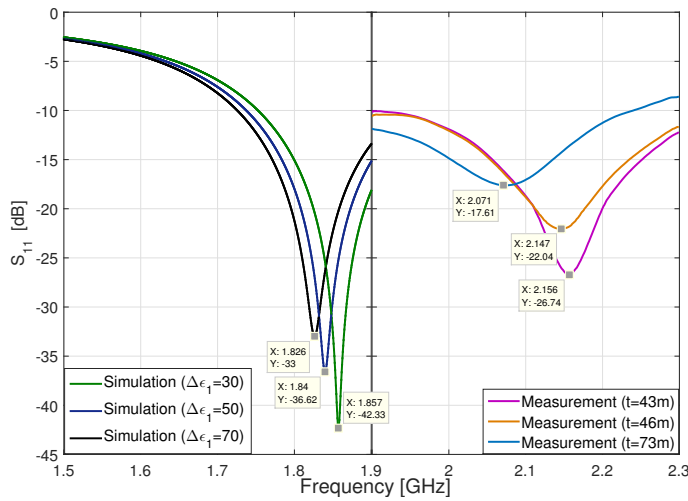
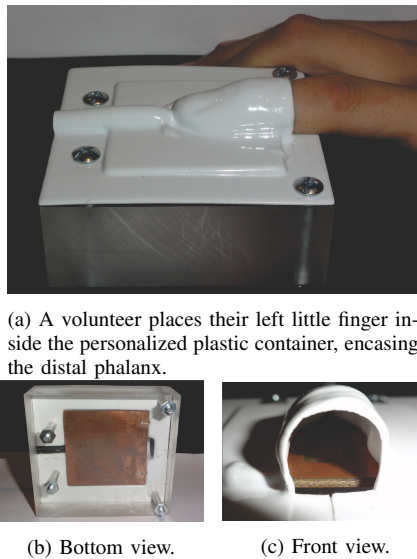


Fig. 11: Spectroscopy comparison of three measured  $S_{11}$  parameter curves and three simulations.



(a) A volunteer places their left little finger inside the personalized plastic container, encasing the distal phalanx.  
(b) Bottom view. (c) Front view.

Fig. 12: Implemented prototype of the proposed GCPW sensor.

glucose. A correlation between both datasets was thus suspected. Figure 14 includes the linear function that best fit the data, using the least-squares criterion. The linearity of the trend was evaluated by calculating the *Pearson* coefficient [35], denoted as “ $r$ ”, which resulted in  $r \approx 0.91$ . A value so close to unity indicates a strong linear relationship between the obtained data. This highlights an interchangeability of these blood glucose measurement methods. The linearity of the trend is noteworthy, and such behaviors have been reported in previous works [14], [17], [20].

The quality factor was studied as another possible parameter of interest. A time line of the blood glucose measurements and corresponding  $Q$  values is shown in Figure 15. In this case, a similarity between the two curves is not apparent. Thus, a correlation between these two datasets cannot be suspected with as much certainty as in the previous case. The *Pearson*

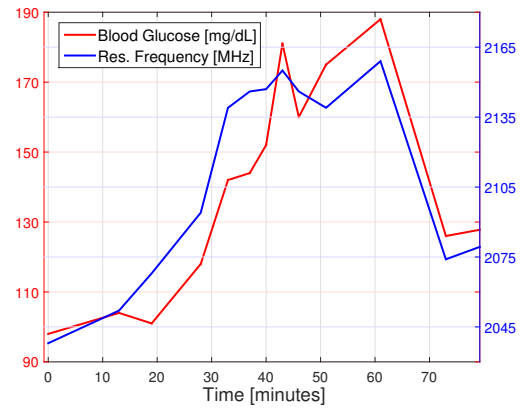


Fig. 13: Resonance frequency (blue) and measured blood glucose levels (red) versus time, during experimental validation.

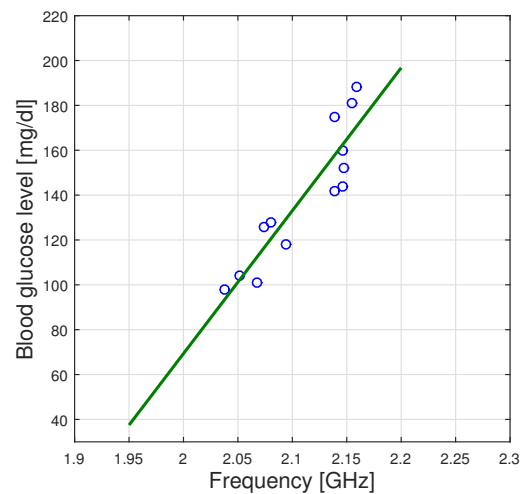


Fig. 14: Measured resonance frequency values and blood glucose levels (circles). Fitting curve obtained via least-squares criterion (green).

coefficient for these curves results in  $r \approx 0.64$ . This was deemed inconclusive, and so the resonance frequency was selected as the main parameter to be measured.

Using the regression equation as a calibration curve, a measured resonance frequency can be directly associated with a blood glucose value for this volunteer. This is not necessarily the case for other individuals, since the frequency may be shifted due to finger size and layer thickness, as shown in Table I. Thus, the calibration curve should be personalized. The maximum relative error between the measured data and this calibration curve was of 12%. This is within the standard  $\pm 15\%$  error considered acceptable for blood glucose measurements. However, a clinical procedure utilizing an error-free blood glucose reading instead of a traditional glucometer as reference would be needed in order to re-calibrate this curve.

The slope of the linear equation in Figure 14 is equal to the average frequency shift resulted from a change in blood glucose during the experiment. This is a measure of how

TABLE II: Performance comparison of the proposed sensor with previously published works.

Reference	Frequency shift [kHz] per mg/dL of change	Technology	Position Error [MHz]	Human Tested Variation [mg/dL]	Modeled Variation [mg/dL]	Resolution [mg/dL]	Max. error in testing
Proposed	1340	Non-invasive. Fingertip placed on planar resonator.	< 100	98 – 188	0 – 16000	0.75	12%
[14]	14	Same as above.	< 150	N.A.	100 – 500	N.A.	N.A.
[15]	240	Same as above.	< 130	137 – 339	105 – 500	4	32%
[16]	2.81	Same as above.	< 15	N.A.	0 – 16000	N.A.	N.A.
[19]	62.5	Invasive. Resonator senses properties of extracted microfluid.	–	N.A.	0 – 8000	N.A.	N.A.
[20]	0.5	Non-invasive. Wearable split-ring resonator.	–	80 – 150	0 – 4000	0.6	N.A.
[21]	1990	Invasive. Samples placed directly on planar resonator.	–	92 – 120	25 – 500	N.A.	< 1%

N.A. = Not Available. The dash (–) is used to indicate that the comparison is not applicable to a case, due to difference of technology or approach.

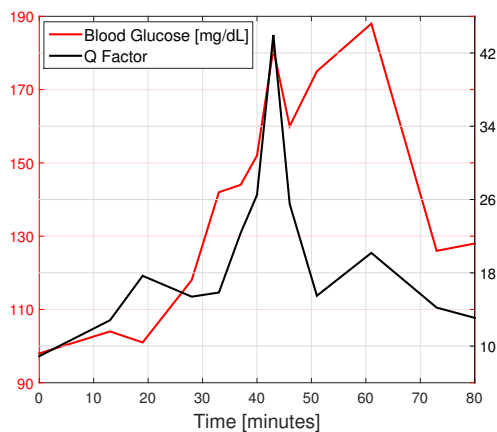


Fig. 15: Quality factor (black) and measured blood glucose levels (red) versus time, during experimental validation.

sensitive the sensor is to the blood glucose of the user. In this case, the slope resulted in 1340 kHz/(mg/dL), which is comparable with the 1990 kHz/(mg/dL) reported in [21] which utilized an invasive technique. The proposed sensor was more sensitive, by at least an order of magnitude, than other non-invasive sensors developed in the recent literature [14]–[16], [20], which reported average slopes of 14, 240, 2.81 and 0.5 kHz/(mg/dL), respectively. This is attributed to the considerable volume of the finger that interacts with the sensor (including the totality of the distal phalanx on the sensor, and not just the fingertip) and the lower frequency employed, which favors tissue penetration and the interaction of the microwaves with the blood tissue.

The minimum change in blood glucose that could be detected by this sensor is a measure of the resolution of the

prototype. This can be estimated from the experimental data. The discrimination of closely spaced frequency components in the utilized SA (i.e. the resolution bandwidth) is determined by the bandpass IF filter, which was set to 1 MHz. Dividing this value by the slope of the experimental curve, the result is the minimum blood glucose change that can be detected (as a 1 MHz shift in resonance frequency). This approximately equals to 0.75 mg/dL for the proposed sensor. This resolution is comparable with the 0.6 mg/dL reported by [20].

Table II includes a performance comparison with the available information in the mentioned previously published works.

#### IV. CONCLUSIONS

A topology for the non-invasive microwave sensing of blood glucose concentration has been proposed. An analysis over three different microwave structures has been performed, and the most suitable one in terms of its frequency sensitivity and the repeatability of its measurements was selected. The experimental performance of the proposed device proved to be encouraging when compared with similar structures found in the literature. The novelty and advantages of the proposed device are highlighted in the high overall sensitivity, the good resolution, the linearity of the correlation, the low relative error, and the non-invasive, reagent-free, real time operation. The high sensitivity was attributed to the considerable volume of the finger in contact with the sensor, and also the lower frequency employed (around 2.1 GHz), favoring tissue penetration and the interaction of the microwaves with the blood tissue. A broader band spectroscopy could provide further information from other resonance modes. It is expected, however, that tissue penetration (hence, sensitivity) should decrease for higher frequencies, due to the loss in the tissues.



Research on the technology should continue in order to find further improvements in the measurement procedure.

Although the simulated resonance frequency showed differences with the final implemented one, the simulations were still valuable to predict the existence of said variation. The discrepancies could be attributed to the multi-layer model of the finger, which remains a simplification of a real one. This model was obtained via ultrasound techniques. Since the thickness of each layer may vary between different users, a statistical analysis over a larger population would be recommended for future improvements of the model.

The addition of a plastic fixing container as part of the measurement equipment improved the invariance with respect to the position of the finger placed on the sensor. This box was designed specifically to fixate the finger of the volunteer, thus achieving more repeatable results. Since there are many factors that can modify the resonance frequency of the resonator-finger system, an individual, learning-based adjustment of the calibration curve could prove useful for a future prototype.

#### ACKNOWLEDGMENT

We earnestly thank María Laura Abait and her colleagues for their aid in the process of measuring layer thicknesses and other characteristics of a human finger by using ultrasound equipment. The data were instrumental in allowing us to construct the model utilized in this research.

We also want to thank CST STUDIO SUITE for facilitating us with an evaluation license for the use of this simulation tool.

Finally, we especially thank the National University of Mar del Plata, and the National Scientific and Technical Research Council (CONICET) for funding this research.

#### REFERENCES

- [1] "International Diabetes Federation (IDF): Diabetes complications," <https://www.idf.org/aboutdiabetes/complications>, accessed: 2020-02-06.
- [2] C. Valeri, P. Pozzilli, and D. Leslie, "Glucose control in diabetes," *Diabetes/metabolism research and reviews*, vol. 20, no. S2, pp. S1–S8, 2004.
- [3] M. Tierney, J. A. Tamada, R. O. Potts, R. C. Eastman, K. Pitzer, N. R. Ackerman, and S. J. Fermi, "The GlucoWatch biographer: A frequent, automatic and noninvasive glucose monitor," *Annals of medicine*, vol. 32, pp. 632–41, 01 2001.
- [4] "SugarBEAT Nemaaura Medical," <https://nemaauramedical.com/sugarbeat/>, accessed: 2020-02-06.
- [5] "Continuous Glucose Measurement: FreeStyle Libre," <https://www.freestylelibre.us/>, accessed: 2020-02-06.
- [6] "The Eversense Difference: Eversense Continuous Glucose Monitoring," <https://www.eversenseddiabetes.com/>, accessed: 2020-02-06.
- [7] "Dexcom Continuous Glucose Monitoring," <https://www.dexcom.com>, accessed: 2020-02-06.
- [8] E. V. Karpova, E. V. Shcherbacheva, A. A. Galushin, D. V. Vokhmyanina, E. E. Karyakina, and A. A. Karyakin, "Noninvasive diabetes monitoring through continuous analysis of sweat using flow-through glucose biosensor," *Analytical Chemistry*, vol. 91, no. 6, pp. 3778–3783, 2019, pMID: 30773009.
- [9] J. Poeze, M. Lamego, S. Merritt, C. Dalvi, H. Vo, J. Bruinsma, F. Lesmana, and M. Joe E Kiani, "Multi-stream data collection system for noninvasive measurement of blood constituents," 06 2016.
- [10] T. Yilmaz, R. Foster, and Y. Hao, "Radio-frequency and microwave techniques for non-invasive measurement of blood glucose levels," *Diagnostics*, vol. 9, no. 1, 2019.
- [11] R. J. Buford, E. C. Green, and M. J. McClung, "A microwave frequency sensor for non-invasive blood-glucose measurement," in *2008 IEEE Sensors Applications Symposium*, Feb 2008, pp. 4–7.

- [12] V. Turgul and I. Kale, "A novel pressure sensing circuit for non-invasive rf/microwave blood glucose sensors," in *2016 16th Mediterranean Microwave Symposium (MMS)*, Nov 2016, pp. 1–4.
- [13] —, "Influence of fingerprints and finger positioning on accuracy of rf blood glucose measurement from fingertips," *Electronics Letters*, vol. 53, no. 4, pp. 218–220, 2017.
- [14] —, "Simulating the effects of skin thickness and fingerprints to highlight problems with non-invasive rf blood glucose sensing from fingertips," *IEEE Sensors Journal*, vol. 17, no. 22, pp. 7553–7560, Nov 2017.
- [15] S. Kiani, P. Rezaei, M. Karami, and R. A. Sadeghzadeh, "Band-stop filter sensor based on siw cavity for the non-invasive measuring of blood glucose," *IET Wireless Sensor Systems*, vol. 9, no. 1, pp. 1–5, 2019.
- [16] M. N. Hasan, S. Tamanna, P. Singh, M. D. Nadeem, and M. Rudramuni, "Cylindrical dielectric resonator antenna sensor for non-invasive glucose sensing application," in *2019 6th International Conference on Signal Processing and Integrated Networks (SPIN)*, March 2019, pp. 961–964.
- [17] R. Baghbani, M. A. Rad, and A. Pourziad, "Microwave sensor for non-invasive glucose measurements design and implementation of a novel linear," *IET Wireless Sensor Systems*, vol. 5, no. 2, pp. 51–57, 2015.
- [18] T. Yilmaz, R. Foster, and Y. Hao, "Broadband tissue mimicking phantoms and a patch resonator for evaluating noninvasive monitoring of blood glucose levels," *IEEE Transactions on Antennas and Propagation*, vol. 62, no. 6, pp. 3064–3075, June 2014.
- [19] D. Mondal, N. K. Tiwari, and M. J. Akhtar, "Microwave assisted non-invasive microfluidic biosensor for monitoring glucose concentration," in *2018 IEEE SENSORS*, Oct 2018, pp. 1–4.
- [20] H. Choi, J. Naylor, S. Luzio, J. Beutler, J. Birchall, C. Martin, and A. Porch, "Design and in vitro interference test of microwave noninvasive blood glucose monitoring sensor," *IEEE Transactions on Microwave Theory and Techniques*, vol. 63, no. 10, pp. 3016–3025, Oct 2015.
- [21] N. Kim, K. Adhikari, R. Dhakal, Z. Chuluunbaatar, C. Wang, and E.-S. Kim, "Rapid, sensitive, and reusable detection of glucose by a robust radiofrequency integrated passive device biosensor chip," *Rapid, sensitive, and reusable detection of glucose by a robust radiofrequency integrated passive device biosensor chip*, vol. 5, 01 2015.
- [22] K. K. Adhikari and N. Kim, "Ultrahigh-sensitivity mediator-free biosensor based on a microfabricated microwave resonator for the detection of micromolar glucose concentrations," *IEEE Transactions on Microwave Theory and Techniques*, vol. 64, no. 1, pp. 319–327, Jan 2016.
- [23] E. Topsakal, T. Karacolak, and E. C. Moreland, "Glucose-dependent dielectric properties of blood plasma," in *2011 XXXth URSI General Assembly and Scientific Symposium*, Aug 2011, pp. 1–4.
- [24] F. Caspers, "Rf engineering basic concepts: S-parameters," 01 2012.
- [25] "Enzyme Hexokinase," [https://www.cdc.gov/nchs/data/nhanes/nhanes\\_03\\_04/110am\\_c\\_met\\_glucose.pdf](https://www.cdc.gov/nchs/data/nhanes/nhanes_03_04/110am_c_met_glucose.pdf), accessed: 2020-02-06.
- [26] G. Martinsen, S. Grimnes, and H. P. Schwan, "Interface phenomena and dielectric properties of biological tissue," 2002.
- [27] M. Hofmann, G. Fischer, R. Weigel, and D. Kissinger, "Microwave-based noninvasive concentration measurements for biomedical applications," *IEEE Transactions on Microwave Theory and Techniques*, vol. 61, no. 5, pp. 2195–2204, May 2013.
- [28] M. Eleiwa and A. Elsherbeni, "Debye constants for biological tissues from 30 hz to 20 ghz," vol. 16, pp. 202–213, 11 2001.
- [29] J. Nuutinen, R. Ikäheimo, and T. Lahtinen, "Validation of a new dielectric device to assess changes of tissue water in skin and subcutaneous fat," *Physiological Measurement*, vol. 25, no. 2, pp. 447–454, feb 2004.
- [30] J. Svacina, "A simple quasi-static determination of basic parameters of multilayer microstrip and coplanar waveguide," *Microwave and Guided Wave Letters*, *IEEE*, vol. 2, pp. 385 – 387, 11 1992.
- [31] "CST Studio Suite (evaluation license)," 2013.
- [32] "FR4 Datasheet," <https://www.farnell.com/datasheets/1644697.pdf>, accessed: 2020-02-03.
- [33] U. Rosenberg and S. Amari, "Novel coupling schemes for microwave resonator filters," *IEEE Transactions on Microwave Theory and Techniques*, vol. 50, no. 12, pp. 2896–2902, Dec 2002.
- [34] D. C. Rebenaque, F. Q. Pereira, J. P. Garcia, A. A. Melcon, and M. Guglielmi, "Two compact configurations for implementing transmission zeros in microstrip filters," *IEEE Microwave and Wireless Components Letters*, vol. 14, no. 10, pp. 475–477, Oct 2004.
- [35] E. S. Pearson, "The test of significance for the correlation coefficient," *Journal of the American Statistical Association*, vol. 26, no. 174, pp. 128–134, 1931.